

# Analysis of the Impact of Clutch-Type Limited Slip Differential on Vehicle Behavior on Slippery Roads

Trung Luong The<sup>1</sup>

<sup>1</sup>Institute of Vehicle & Energy in Transportation Engineering, Le Quy Don Technical University, HaNoi, Vietnam - 10000

**Abstract**—The differential is an important part of the vehicle's powertrain. The symmetrical bevel gear differential has a friction torque-increasing mechanism in the clutch-type Limited Slip Differential (LSD) that improves the vehicle's handling and controllability in various driving conditions, especially on some moving terrains where the grip of the wheels on both sides of the same driving axle is different. The construction of a dynamic calculation model of this differential combined with simulation on Matlab/Simulink software allows a clearer understanding of the operation of the differential assembly, as well as the effect of this type of differential in improving the dynamic properties of the vehicle's movement, especially on roads with poor grip.

**Keywords**— Friction Torque-Increasing, Limited Slip Differential, Slippery road.

## I. INTRODUCTION

The differential in a vehicle is primarily responsible for transmitting torque while allowing the wheels to rotate at different angular velocities. On low-grip road surfaces, the symmetrical bevel gear differential performs effectively. However, under challenging terrain conditions where there is a significant difference in wheel traction, the symmetrical bevel gear differential alone cannot optimize traction or stabilize vehicle motion [1]. To enhance the grip of the driving wheels, increasing the locking coefficient of the differential is necessary. This is typically achieved using either axle differentials or limited slip differentials (LSDs).

Axle differentials provide excellent traction on complex terrains but force both wheels to rotate at the same speed, potentially overloading the transmission system. In contrast, clutch-type limited slip differentials offer greater flexibility in torque distribution, making them more suitable for various driving conditions.

This paper focuses on developing a dynamic model of a clutch-type LSD to evaluate the impact of increased internal friction on vehicle motion. The study establishes the theoretical foundation for the dynamic modeling of an automobile's planar motion equipped with both a symmetrical bevel gear differential and a limited slip differential.

## II. BACKGROUND

### A. Assumption

For simplicity, the following assumptions are made in the model: The steering angles of both front wheels are identical; The tires remain in continuous contact with the ground; The vehicle operates on a uniform, flat surface; The influence of the suspension system is neglected; The front and rear track widths are considered equal, with the center of gravity (CoG)

positioned symmetrically along the vehicle's width; Air resistance and slope resistance are not taken into account.

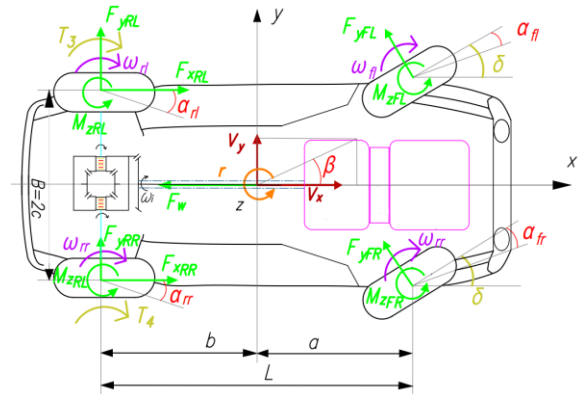


Fig. 1. Simple dynamic model for differential analysis.

Seven degrees of freedom (DOFs) are selected, including:  $q = \{V_x, V_y, r, \omega_{FL}, \omega_{FR}, \omega_{RL}, \omega_{RR}\}$ . Where:  $V_x, V_y$  are velocities of CoG C along the vehicle's longitudinal and lateral axes, respectively;  $r$  is vehicle's yaw rate;  $\omega_{FL}, \omega_{FR}, \omega_{RL}, \omega_{RR}$  represent the rotational velocities of the left front wheel, right front wheel, left rear wheel, and right rear wheel, respectively.

### B. Tire model

Tire model is used to analyze the interaction between the tires and the road. In this paper, we use the 1997 version of the Pacejka model. The magic formula is represented as in (1):

$$(F_{xi}, F_{yi}, M_z) = PAC1997(\kappa_i, \alpha_i, F_{zi}) \quad (1)$$

Another form of the formula is represent in (2):

$$y = D \sin[C \arctan\{Bx - E(Bx - \arctan Bx)\}] \quad (2)$$

Where:  $Y(X) = y(x) + S_v, x = X + S_H$

$$V_{sx} = V_x - V_r; \quad V_{sy} = V_y;$$

$$\kappa = -\frac{V_{sx}}{V_x} = -\frac{V_x - R_e \cdot \omega}{V_x}; \quad \tan \alpha = \frac{V_{sy}}{|V_x|}$$

$B, C, D, E$  are stiffness factor, shape factor, peak value, curvature factor, respectively.  $S_H$  denotes lateral shift and  $S_V$  represents longitudinal shift.

The effect of the camber angle as well as the  $M_x$  component is neglected. The parameters of each wheel are determined as follows:

\* Longitudinal slip  $\kappa$ :

Longitudinal slip is calculated using constant  $\varepsilon = 0.01$  to avoid division by 0 as shown in (3):

$$\begin{cases} \kappa_i = \frac{R_e \omega_i - V_{xi}}{\max(V_{xi}, \varepsilon)}; \\ i = \{FL, FR, RL, RR\}; \varepsilon = 0.01; \end{cases} \quad (3)$$

Longitudinal velocities of wheels are calculated as in (4):

$$\begin{cases} V_{xFL} = (V_x - c.r)\cos(\delta) + (V_y + a.r)\sin(\delta); \\ V_{xFR} = (V_x + c.r)\cos(\delta) + (V_y + a.r)\sin(\delta); \\ V_{xRL} = V_x - c.r; \\ V_{xRR} = V_x + c.r; \end{cases} \quad (4) \quad V_y \approx \beta V_x$$

Where:  $V_{xi}$  is longitudinal velocity along (Ox)w axis;  $r$  is calculation radius;  $\omega_i$  is rotational velocity of wheel  $i$ ;  $a$  is distance from CoG C to front axle;  $c = B/2$ ,  $B$  is front track of a vehicle.

\* Side slip angle  $\alpha$  :

Side slip angle can be calculated as in (5):

$$\alpha_i = \delta_i - \beta_i = \delta_i - \arctan\left(\frac{V_{yi}}{V_{xi}}\right) = \delta_i - \arctan\left(\frac{V_y + x_i r}{V_x - y_i r}\right) \quad (5)$$

Where:

$\delta_i$  is steer angle;

$\beta$  is attitude angle;

$V_{xi}$ ,  $V_{yi}$  are vehicle's longitudinal and lateral velocities  
( $x_i$ ,  $y_i$ ) is position of wheel frame in body frame  $B(Cxyz)$

From (5), we get side slip angle of front wheels and rear wheels as in (6):

$$\Rightarrow \begin{cases} \alpha_{FL} = \delta - \arctan\left(\frac{v_y + a.r}{v_x - c.r}\right) & \alpha_{FR} = \delta - \arctan\left(\frac{v_y + a.r}{v_x + c.r}\right) \\ \alpha_{RL} = -\arctan\left(\frac{v_y - b.r}{v_x + c.r}\right) & \alpha_{RR} = -\arctan\left(\frac{v_y - b.r}{v_x - c.r}\right) \end{cases} \quad (6)$$

\* Vertical reaction forces:

According to [4], vertical reaction forces can be calculated as in (7):

$$\begin{cases} F_{zFL} = mg \cdot \frac{b}{2l} \cdot \left(1 - \frac{h}{b} \cdot \frac{a_x}{g}\right) \cdot \left(1 - \frac{h}{c} \cdot \frac{a_y}{g}\right) & F_{zRL} = mg \cdot \frac{a}{2l} \cdot \left(1 + \frac{h}{a} \cdot \frac{a_x}{g}\right) \cdot \left(1 - \frac{h}{c} \cdot \frac{a_y}{g}\right) \\ F_{zFR} = mg \cdot \frac{b}{2l} \cdot \left(1 - \frac{h}{b} \cdot \frac{a_x}{g}\right) \cdot \left(1 + \frac{h}{c} \cdot \frac{a_y}{g}\right) & F_{zRR} = mg \cdot \frac{a}{2l} \cdot \left(1 + \frac{h}{a} \cdot \frac{a_x}{g}\right) \cdot \left(1 + \frac{h}{c} \cdot \frac{a_y}{g}\right) \end{cases} \quad (7)$$

Newton-Euler equations of motion for the vehicle are shown in (8):

$$\begin{cases} m(\dot{V}_x - V_y r) = F_x - F_w \\ m(\dot{V}_y + V_x r) = F_y \\ M_z = I_z \dot{r} \quad (r = \omega_z) \end{cases} \quad (8)$$

By expressing (8) in vehicle's body coordinate, we have (9):

$$\begin{cases} F_x = (F_{xFL} + F_{xFR})\cos\delta + (F_{xRL} + F_{xRR}) - (F_{yFL} + F_{yFR})\sin\delta \\ F_y = (F_{xFL} + F_{xFR})\sin\delta + (F_{yFL} + F_{yFR})\cos\delta + (F_{yRL} + F_{yRR}) \\ M_z = ((F_{xFL} + F_{xFR})\sin\delta + (F_{yFL} + F_{yFR})\cos\delta)a - (F_{yRL} + F_{yRR})b \\ + (-F_{xFL}\cos\delta + F_{yFL}\sin\delta + F_{xFR}\cos\delta - F_{yFR}\sin\delta - F_{xRL} + F_{xRR})c \\ + (M_{zFL} + M_{zFR} + M_{zRL} + M_{zRR}) \end{cases} \quad (9)$$

According to [3], aerodynamic force is calculated as in (10):

$$F_w = 0.5 \cdot \rho_w \cdot C_w \cdot S \cdot V_x^2 = k_w \cdot S \cdot V_x^2 \quad (10)$$

Where:  $\rho_w$  is air's density (we choose  $\rho_w = 1,225 \text{ kg/m}^3$  at normal condition),  $k_w = 0,6125 \cdot C_w$  [kg/m<sup>3</sup>] is drag coefficient,  $C_w$  is total aerodynamic coefficient (for passenger cars,  $C_w = 0,5$ ).

### C. Dynamics tire equations

A dynamic tire model is represented in Fig. 2.

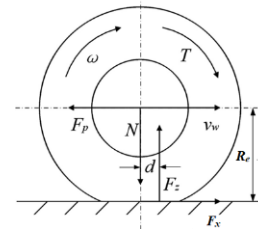


Fig. 2. Simple dynamic model for differential analysis.

According to the model, we have (11):

$$\begin{aligned} I_w \dot{\omega}_i &= T_i - R_e \cdot F_{xi} - d \cdot F_{zi} = R_e \left( \frac{T_i}{R_e} - F_{xi} - \frac{d}{R_e} F_{zi} \right) \\ \Leftrightarrow \dot{\omega}_i &= \frac{R_e}{I_w} \left( \frac{T_i}{R_e} - F_{xi} - f \cdot F_{zi} \right) \end{aligned} \quad (11)$$

Where:  $F_x$  is calculated using PAC 1997 model [2],  $R_e$  is wheel's dynamic radius and it is constant (it is the same for all wheels),  $F_z$  is the total vertical reaction force applied at tireprint,  $d$  is deformation of  $F_z$  from the initial position,  $f = d/R_e$  is rolling resistance coefficient (in this paper, we assume that it is constant),  $T_f = F_z \cdot d$  is rolling resistance moment.

### D. Dynamic equations of differential

According to [5], the power calculation equations are:

$$\begin{aligned} \dot{W}_{loss} &= -(P_t + P_d + P_c) + P_s \\ P_t &= \eta(T_d \omega_d + T_1 \omega_1 + T_2 \omega_2) \\ P_d &= -(b_1 |\omega_1| + b_2 |\omega_2| + b_d |\omega_d|) \\ P_c &= T_c |\bar{\omega}| \\ P_s &= -(\omega_1 \dot{\omega}_1 J_1 + \omega_2 \dot{\omega}_2 J_2 + \omega_d \dot{\omega}_d J_d) \end{aligned} \quad (12)$$

The differential dynamic equations of the ring gear:

$$\dot{\omega}_d J_d = \eta T_d - \omega_d b_d - T_i \quad (13)$$

Equations of the left axle shaft:

$$\dot{\omega}_1 J_1 = \eta T_1 - \omega_1 b_1 - T_{i1} \quad (14)$$

Equations of the right axle shaft:

$$\dot{\omega}_2 J_2 = \eta T_2 - \omega_2 b_2 - T_{i2} \quad (15)$$

Assuming that the connection between the ring gear and the axle shafts is perfectly rigid, the constraint equations are applied:

$$\begin{aligned} \eta T_1 &= \frac{N}{2} T_{ioi} - \frac{1}{2} T_c \\ \eta T_2 &= \frac{N}{2} T_{ioi} + \frac{1}{2} T_c \\ \omega_d &= \frac{N}{2} (\omega_1 + \omega_2) \end{aligned} \tag{16}$$

III. EXPERIMENTAL MODEL

A. Experiment configuration

The experimental diagram is built as in Fig. 3.

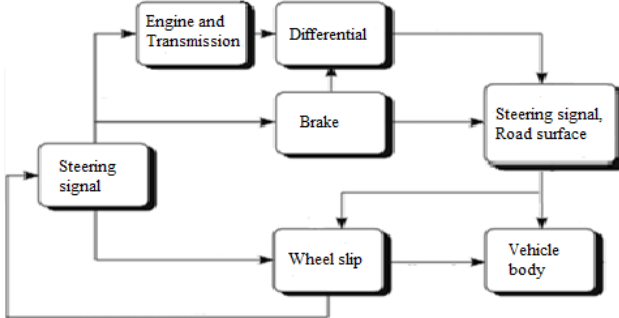


Fig. 3. Experimental diagram.

We use Matlab/Simulink to examine dynamics differential. The input data are determined as shown in Table I.

TABLE I. Input data for the experiment.

S. No.	Specifications	Value	Unit
Vehicle's basic specifications			
1	Total length	4857	mm
	Total width	2197	mm
	Total height	1776	mm
	Wheel base	2983	mm
	Weight	2105	Kg
	Weight distribution on front axle	1284	Kg
	Weight distribution on rear axle	821	Kg
	Drivetrain	RWD	
	Maximum Power	220	kW
	Maximum Torque	1500	Nm
	Maximum rotation speed	6000	rpm
	Distance from CoG to front axle	1.4	m
	Distance from CoG to rear axle	1.6	m
	Height of CoG	0.5	m
Friction disc specifications			
	Number of friction surfaces	6	
	Outer radius of the friction surface	30	mm
	Inner radius of the friction surface	10	mm
	Coefficient of static friction	0.25	
	Coefficient of dynamic friction	0.2	

B. Results

To understand how effective is LSD, we comparing the operation of LSD to an open differential. The results has been shown in Fig. 4. And Fig. 5.

Under the given condition where the road surface has different grip levels between the two sides of the wheel, the friction-enhancing differential demonstrates superior torque transmission and traction optimization on the driven axle compared to the conventional symmetrical bevel gear

differential. In practice, the bevel gear differential still fulfills its secondary function effectively, as most of the time, vehicles operate on roads with good traction. However, with advancements in modern technology and continuous development, the limited-slip differential emerges as a promising direction. With its advantages, including an automatic mechanism, improved power transmission efficiency, simple design, and high durability, the disc-type friction-enhancing differential can be a valuable solution for military vehicles.

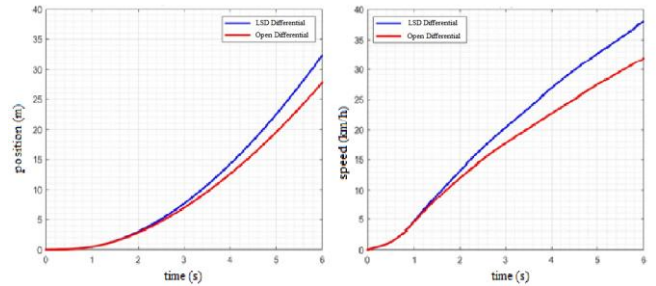


Fig. 4. Position and speed of the two types of differentials during operation.

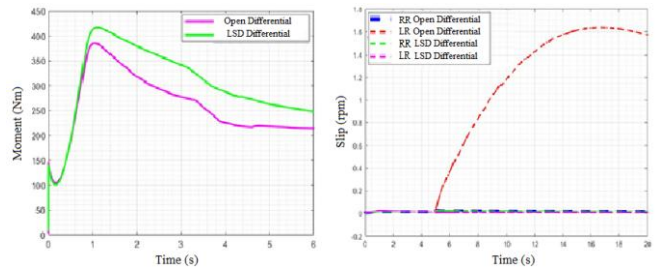


Fig. 5. Driven axle torque and slip ratio comparison between two types of differentials.

IV. CONCLUSION

This paper has developed a dynamic model for the movement of a vehicle equipped with two differentials. The simulation results demonstrate consistency with the actual motion of the utility vehicle as well as with the established methods. Although the assumed conditions are overly idealized and the road conditions do not fully reflect real-world scenarios, the simulation results still provide valuable insights into the dynamic behavior and the traction enhancement effects of the friction-increasing differential.

REFERENCES

- [1] P. Kopf, M. Escher, U. Gazyakan, and M. Oberhauser, "Optimization of traction and driving stability in 2-wheel drive cars by means of electro-hydraulic limited-slip differentials," in *SAE Technical Paper Series*, 1990, paper no. 905108.
- [2] H. B. Pacejka, *Tyre and Vehicle Dynamics*, 2nd ed. SAE International, 2005.
- [3] R. N. Jazar, *Vehicle Dynamics: Theory and Application*. Springer International Publishing, 2017.
- [4] R. N. Jazar, *Advanced Vehicle Dynamics*. Springer International Publishing, 2019.
- [5] H. B. Pacejka, *Tyre and Vehicle Dynamics*, 2nd ed. SAE International, 2005.
- [6] R. H. Haas, "Development of a Limited Slip Differential," Rep. 1971.